

The effects of deformation and pairing correlations on nuclear charge form factor

Ch. C. Moustakidis¹, T. S. Kosmas^{1,2}, F. Simkovic^{1,3} and Amand Faessler¹

¹*Institute of Theoretical Physics, University of Tuebingen,
D-72076 Tuebingen, Germany*

²*Theoretical Physics Division, University of Ioannina,
GR-45110 Ioannina, Greece*

³*Department of Nuclear Physics, Comenius University,
SK-84215 Bratislava, Slovakia*

Abstract

A set of moderately deformed $s - d$ shell nuclei is employed for testing the reliability of the nuclear ground state wave functions which are obtained in the context of a BCS approach and offer a simultaneous consideration of deformation and pairing correlations effects. In this method, the mean field is assumed to be an axially symmetric Woods-Saxon potential and the effective two-body interaction is a monopole pairing force. As quantities of main interest we have chosen the nuclear form factors, the occupancies of the active (surface) orbits and the Fermi sea depletion, which provide quite good tests for microscopic descriptions of nuclei within many body theories. For our comparisons with results emerging from other similar methods, an axially deformed harmonic oscillator field is also utilized.

PACS : 21.60.Jz, 23.40.Hc, 27.30+t, 21.10 Ft

1 Introduction.

In recent nuclear structure calculations, the reliability of various predictions associated with phenomena of several prominent electroweak processes (β -decay modes, lepton-capture by nuclei, neutrino-nucleus reactions, etc.) relies upon the accurate description of the nuclear many-body wave functions [1, 2]. Among the nuclear structure aspects which can quite strongly influence such predictions, the consideration of the deformation [3, 4, 5, 6] and the nucleon-nucleon correlations effects [7, 8, 9, 10] (wherever they might be appreciable) is of significant importance. As it is well known, the ground state nucleon-nucleon correlations [7] are of particular significance to be reliably incorporated especially when investigating processes for which the branching ratios or decay (event) rates are highly suppressed and, therefore, the corresponding transition matrix elements are very sensitive [5, 8]. Moreover, the nuclear deformation, e.g. for axially symmetric nuclear systems, should necessarily be considered by applying appropriate treatments and using reliable methods [3, 4, 5, 6].

The main purpose of the present work is to address the effects of deformation and pairing correlations on a few nuclear observables of the ground state for moderately deformed s-d shell nuclei in the spirit of approaches based on BCS quasi-particles. The properties of main interest are the ground state charge form factor $F_{ch}(\mathbf{q})$ [11, 12, 13, 14, 15], as well as the occupancy (vacancy) numbers of several orbitals around the Fermi level [16, 17, 18, 19, 20]. Such quantities (also those referred to low-lying excitations like transition densities, transition form factors, etc.) constitute very common tests in nuclear structure theory for the many-body model wave functions [1, 16]. Experimentally, the above properties are known with very high accuracy ($\approx 1\%$), e.g. from experiments of elastic scattering of electrons, protons, etc. off target nuclei [11, 12, 13, 14]. On the theoretical side, average potentials (spherical Woods-Saxon or harmonic oscillator, etc.) employed in BCS theories and nucleon orbitals, both of which are directly related to gross nuclear features of the ground states, have been quite effective in describing the dynamics of many mainly spherical nuclei [10, 17, 20, 21]. However, even though the direct calculation of the charge form factor (and other gross nuclear properties) through a nuclear model ground state (g.s.) wave function is a very extensively discussed issue, the reproducibility of the scattering data in the high momentum transfer region ($q > 2-3 \text{ fm}^{-1}$) with the experimental accuracy has not yet been achieved (in the context of any nuclear model) for

most of the nuclear systems.

The existence of nuclear deformation, in general, is closely related to the non-spherical components of the proton (neutron) density distribution and the corresponding proton (neutron) nuclear form factor whereas the nucleon-nucleon correlations are, to a large extent, related to the nuclear surface texture, the main characteristics of which are the occupation probabilities of the active orbits. These quantities are studied in single-nucleon transfer reactions [18], but often the results differ substantially from the predictions of independent particle approximations and other methods, due to the fact that, in many of these models, the correlations and deformation phenomena are not (or may not correctly [22]) taken into account [7]. Hence, details of the nuclear surface and also bulk phenomena for many nuclei may have not correctly been understood in terms of many existing models.

The present method employs a BCS ground state built out of a deformed WS basis wave functions. The required two-body interaction is taken to have a schematic-type, the monopole part of which is scaled phenomenologically (separately for protons and neutrons) so as to be consistent with the observed proton and neutron separation energies within the BCS procedure [5, 23]. At first, we study the nuclear form factors for the set of deformed nuclei $^{24}_{12}\text{Mg}$, $^{26}_{12}\text{Mg}$, $^{28}_{14}\text{Si}$ and $^{32}_{16}\text{S}$ (s-d shell nuclei), by considering them as systems having axially symmetric β (quadrupole) deformation only [24, 25]. They are rather well deformed isotopes with the following values of the parameter β : $\beta(^{24}\text{Mg}) = 0.416$ [25] (0.374 [24]), $\beta(^{26}\text{Mg}) = 0.296$ [25] (-0.310 [24]), $\beta(^{28}\text{Si}) = -0.328$ [25] (-0.478 [24]) and $\beta(^{32}\text{S}) = 0.186$ [25] (0.000 [24]). In the present work we apply also values of the deformation parameter β which originated from experimental values of the quadrupole moment, taken from Ref. [26].

We next proceed with the study of the effects of deformation and pairing interactions on the surface features of these nuclei, namely, on the smearing of their Fermi surface which is very sensitive to the orbit occupancies of the active space. In our method, deformation effects and pairing correlations for proton-proton and neutron-neutron interactions may simultaneously and in a quite reliable manner be considered which is in accord with the experimental indications of Ref. [14] showing that these effects must be treated as much as possible on equal footing. Finally, for the sake of comparison with the results of other similar methods, we study the same properties for the above isotopes, but now by expanding the required deformed Woods-Saxon wave functions into a deformed harmonic oscillator (DHO) basis.

We remark that, spherical WS potentials parameterized for the well depth, skin thickness, radius and spin-orbit constants, etc. as in Ref. [27], have been used by us in the past for microscopic random phase approximation (RPA) calculations of decay (event) rates in electroweak processes ($\beta\beta$ -decay [2], flavor violating processes [8, 21], etc.) for various nuclei. Several of these calculations must be extended to non-spherical systems or must be corrected to include deformation and/or correlations effects. The present method offers some advantages for such purposes [28, 29].

In the remainder of the paper, we first describe the main ingredients of our method (Sect. 2), then we present the results obtained and compare them with existing experimental data (Sect. 3), and finally (Sect. 4) we summarize the main conclusions extracted.

2 Brief description of the formalism

2.1 Axially symmetric Harmonic Oscillator and Wodds-Saxon bases

For the description of axially symmetric nuclear systems, where the cylindrical coordinates (r, z, ϕ) are appropriate, a deformed harmonic oscillator (DHO) potential has been primarily used [30]. The eigenfunctions of this unharmonic oscillator are described in terms of two frequencies: ω_z , in the direction of the z-axis, and ω_{\perp} , for the motion perpendicular to the symmetry z-axis. Then, the space-spin DHO single particle wave functions are written as [30]

$$\Psi_{n_{\rho}, n_z, \Lambda, \Sigma}(\mathbf{r}, \sigma) \equiv \Psi_{n_{\rho}, n_z, \Lambda, \Sigma}(\rho, z, \phi, \sigma) = \psi_{n_{\rho}}^{|\Lambda|}(\rho) \psi_{n_z}(z) \psi_{\Lambda}(\phi) \chi(\Sigma) \quad (1)$$

where Σ and Λ are the projections on the z-axis of the spin and orbital angular momentum, respectively. $\chi(\Sigma)$ stands for the spin wave function and the components of the spatial parts are defined as follows:

(i) The radial part is usually written in terms of a dimensionless coordinate η defined by

$$\eta = R_{\perp}^2 \rho^2, \quad R_{\perp} = \left(\frac{m\omega_{\perp}}{\hbar}\right)^{\frac{1}{2}}, \quad (2)$$

(m is the nucleon mass) as

$$\psi_{n_{\rho}}^{|\Lambda|}(\rho) = N_{n_{\rho}}^{|\Lambda|} \left(\frac{2m\omega_{\perp}}{\hbar}\right)^{\frac{1}{2}} \eta^{\frac{|\Lambda|}{2}} e^{-\frac{\eta}{2}} L_{n_{\rho}}^{|\Lambda|}(\eta), \quad (3)$$

where

$$N_{n_\rho}^{|\Lambda|} = \left(\frac{n_\rho!}{(n_\rho + |\Lambda|)!} \right)^{\frac{1}{2}}, \quad (4)$$

is a normalization factor and $L_{n_\rho}^{|\Lambda|}(\eta)$ are the associated Laguerre polynomials.

(ii) The z-dependent part is similarly written in terms of a dimensionless variable ξ

$$\xi = R_z z, \quad R_z = \left(\frac{m\omega_z}{\hbar} \right)^{\frac{1}{2}}, \quad (5)$$

as

$$\psi_{n_z}(z) = N_{n_z} \left(\frac{m\omega_z}{\hbar} \right)^{\frac{1}{4}} e^{-\frac{\xi^2}{2}} H_{n_z}(\xi) \quad (6)$$

where again

$$N_{n_z} = (\sqrt{\pi} 2^{n_z} n_z!)^{-\frac{1}{2}}, \quad (7)$$

is a normalization factor and $H_{n_z}(\xi)$ are the Hermite polynomials.

(iii) the ϕ -dependent part is given by

$$\psi_\Lambda(\phi) = \frac{1}{\sqrt{2\pi}} e^{i\Lambda\phi}, \quad (8)$$

which is normalized to unity.

The coordinate scaling parameters R_\perp and R_z , which have dimensions of inverse length, characterize the motion in the perpendicular and z-direction, respectively. Obviously, the level of anisotropy of the field is represented by the difference between the two frequencies, ω_\perp and ω_z , which are written in terms of the usual quadrupole deformation parameter β as [30]

$$\omega_z = \omega_0(\beta) \left(1 - \frac{2}{3}\beta \right), \quad \omega_\perp = \omega_0(\beta) \left(1 + \frac{1}{3}\beta \right)$$

where ω_0 is weakly dependent on β (enough to conserve the nuclear volume). From the latter two equations we obtain

$$\beta = (\omega_\perp - \omega_z)/\omega_0.$$

The parameter β is defined so that $\beta > 0$ correspond to the so-called prolate shapes and $\beta < 0$ correspond to oblate shapes.

The eigenfunctions of the Hamiltonian involving an axially symmetric Woods-Saxon potential have a good quantum number K , the projection of the total angular momentum, $\mathbf{J} = \mathbf{L} + \mathbf{S}$, on the symmetry z-axis, i.e. $K = \Lambda + \Sigma$ (due to the assumed symmetry they are eigenfunctions of the \hat{J}_z

operator). These eigenfunctions can be expanded into basis functions like those of Eq. (1), namely, into the eigenfunctions of a deformed harmonic oscillator potential. In the intermediate region of the parameter β we are interested in, $0.15 \leq \beta \leq 0.50$, one could employ either Eq. (1) or total angular momentum coupled bases like the $\Psi(N, n_z, \Lambda, K)$ (see Ref. [30] p. 118) which we apply in this work (here the principal quantum number N is defined as $N = n_z + 2n_\rho + |\Lambda|$). In this case the expansion of the WS basis takes the form

$$\begin{aligned} \Phi_i(K) &= \sum_{N, n_z, \Lambda} \alpha_i(N, n_z, \Lambda) \Psi(N, n_z, \Lambda, \Sigma = 1/2, K) \\ &+ \sum_{N', n'_z, \Lambda'} \alpha'_i(N', n'_z, \Lambda') \Psi(N', n'_z, \Lambda' = \Lambda + 1, \Sigma' = -1/2, K) \end{aligned} \quad (9)$$

where α_i and α'_i are expansion coefficients obtained from the diagonalization procedure. The time-reversed partners of the states (9) have the form

$$\begin{aligned} \tilde{\Phi}_i(K) &= \sum_{N, n_z, \Lambda} \alpha_i(N, n_z, \Lambda) \Psi(N, n_z, -\Lambda, \Sigma = -1/2, -K) \\ &- \sum_{N', n'_z, \Lambda'} \alpha'_i(N', n'_z, \Lambda') \Psi(N', n'_z, \Lambda' = -\Lambda - 1, \Sigma' = 1/2, -K) \end{aligned} \quad (10)$$

Using Eqs. (9) and (10), we can write the expression for the point proton density distribution in an axially symmetric nucleus as

$$\rho(\mathbf{r}) = \sum_i V_{pi}^2 [\Phi_i^*(K) \Phi_i(K) + \tilde{\Phi}_i^*(K) \tilde{\Phi}_i(K)] \quad (11)$$

where V_{pi}^2 stands for the occupation probability of the i^{th} proton state (in the deformed basis), determined from the solutions of the BCS equations. The proton density distribution, $\rho(\mathbf{r})$, Eq. (11), is related to the proton form factor $F(\mathbf{q})$ of the nucleus in question by the well known expression (Born approximation)

$$F(\mathbf{q}) = \int \rho(\mathbf{r}) e^{i\mathbf{qr}} d\mathbf{r} \quad (12)$$

By choosing \mathbf{q} in the direction of \hat{z} we have, $i\mathbf{qr} = iqr \cos \theta = iqz$. Under this assumption, the nuclear form factor, Eq. (12), can be written in the form

$$F(q) = 2 \sum_i \left(\sum_{N, n_z, \Lambda} \sum_{N', n'_z} \alpha_i(N, n_z, \Lambda) \alpha_i(N', n'_z, \Lambda) I(n_z, n'_z, q) \delta_{n_\rho, n'_\rho} \right) V_{pi}^2 \quad (13)$$

where

$$I(n_z, n'_z, q) = \int_{-\infty}^{\infty} \psi_{n_z}^*(z) \psi_{n'_z}(z) e^{iqz} dz. \quad (14)$$

The first part of our calculations in the present work (see Sect. 3) relies upon Eqs. (13) and (14).

2.2 The BCS model

The ground state of even-even deformed nuclei is determined by the deformed pairing Hamiltonian, which includes monopole proton-proton and neutron-neutron pairing interactions as [5, 31]

$$\begin{aligned} H = & \sum_s (\epsilon_{ps}^0 - \lambda_p) \sum_{\sigma} c_{ps\sigma}^\dagger c_{ps\sigma} + \sum_s (\epsilon_{ns}^0 - \lambda_n) \sum_{\sigma} c_{ns\sigma}^\dagger c_{ns\sigma} \\ & - G_{pp} \sum_{s,s'} S_{spp}^\dagger S_{s'pp} - G_{nn} \sum_{s,s'} S_{snn}^\dagger S_{s'nn}, \end{aligned} \quad (15)$$

where ϵ_{ps}^0 and ϵ_{ns}^0 are the un-renormalized single particle energies for protons and neutrons, respectively. λ_p (λ_n) is the proton (neutron) Fermi energy and the operator $S_{s\tau\tau'}^\dagger$ creates pairs in time reversed orbits written as

$$S_{spp}^\dagger = \sum_{\sigma} c_{ps\sigma}^\dagger c_{ps\tilde{\sigma}}^\dagger, \quad S_{snn}^\dagger = \sum_{\sigma} c_{ns\sigma}^\dagger c_{ns\tilde{\sigma}}^\dagger. \quad (16)$$

Here, $c_{\tau s\sigma}^\dagger$ and $c_{\tau s\sigma}$ stand for the creation and annihilation operators of a particle ($\tau = p$ and $\tau = n$ denote proton and neutron, respectively) in the axially symmetric Woods-Saxon potential. σ is the sign of the angular momentum projection K , namely, $\sigma = \pm 1$. We note that the intrinsic states are twofold degenerate, since the states with K and $-K$ have the same energy as a consequence of the time reversal invariance (the symbol \sim indicates time reversed states). The pairing interaction strengths G_{pp} and G_{nn} , which characterize the associated monopole interaction for proton or neutron pairs, respectively, are determined by fitting the theoretical pairing gaps to the average empirical ones parameterized as, $\Delta_{pp} = \Delta_{nn} = 12.84/A^{1/2}$ MeV [23], where A represent the mass number of the isotope in question.

3 Results and Discussion

The first part of the present calculations refers to the proton form factors of the deformed nuclei $^{24}_{12}\text{Mg}$, $^{26}_{12}\text{Mg}$, $^{28}_{14}\text{Si}$ and $^{32}_{16}\text{S}$ carried out as follows. At first,

in the spirit of the independent particle approximation (Slater determinant calculations), we used a deformed Woods-Saxon field parameterized as in Ref. [27] (in this step there is no correlations effect). In the second step, the pairing correlations are inserted in our calculation by means of the BCS theory, namely through the monopole pairing interaction, a schematic type nucleon-nucleon force. The strength of this pairing force, is determined separately for protons and neutrons as in Ref. [5] (see Sect. 2.2). In the third step of the calculational procedure, for comparison, we evaluated the same proton form factors utilizing now a deformed harmonic oscillator basis in the BCS ground state, as discussed in Sect. 2. Thus, the latter results include correlations of the same kind as those of the second step. For all the cases studied, we adjusted the parameter R_z of Eq. (5) so as, for each isotope, the first diffraction minimum of the nuclear form factor to appear at the experimental position (value of the momentum transfer q). For the deformation parameter β , throughout this part of work we used the more recent calculations of Ref. [25], which are, generally, in agreement with the predictions of the macroscopic-microscopic model of Ref. [24].

The results obtained as described above, are presented in Fig. 1, where we use the notation WS to denote the deformed (axially symmetric) Woods-Saxon results, the notation WS+BCS to represent the results containing in addition pairing correlations, and the notation DHO+BCS for the results which consider the deformation and pairing-correlations effects through the harmonic oscillator model. The main conclusions stemming out of the above calculations are the following. As can be seen from Fig. 1, the incorporation of pairing correlations (second step) via the BCS procedure, affects appreciably the shape of the charge form factors (compare the plots corresponding to WS and WS+BCS results), especially for $q > 2 \text{ fm}^{-1}$, which is a well known outcome. Furthermore, the simultaneous consideration of deformation and pairing correlations in the BCS ground state with Woods-Saxon potential, reproduces the experimental form factor data (and charge density distribution) much better than the deformed harmonic oscillator model (compare results labeled WS+BCS and DHO+BCS). As it is evident from Fig. 1, nearly all the diffraction minima of the results labeled WS+BCS are produced quite close to their experimental momentum transfer locations (also some additional minima not observed by experiments up to now are predicted for values of $q > 3 - 4 \text{ fm}^{-1}$) [20]. For high momentum transfer (close to the nuclear center of the charge density distribution) the reproducibility becomes worse due to the presence of other sorts of correlations not included in our

results (short range nucleon-nucleon correlations, etc.) and other kinds of effects (meson-exchange corrections, etc.).

We investigate also the effect of the deformation on charge form factors as well the occupancy numbers by using various values of the deformation parameter β which originated from Ref. [26] (see also Table 1). More specifically the parameter β calculated through the relation

$$\beta = \sqrt{\frac{\pi}{5}} \frac{Q_0}{Z r_c^2} \quad (17)$$

where Q_0 is the intrinsic quadrupole moment (in barn), r_c is the charge radius (in fm) and Z the number of the proton. Q_0 calculated from the experimental quadrupole moment Q via the relation

$$Q_0 = -\frac{7}{2}Q$$

The relative values are exhibited in Table 1.

Fig. 2 focuses on the nucleus ^{24}Mg and ^{32}S showing the calculated nuclear form factors for various values of the deformation parameter β where taken for Table 1. We see that, the shape of the form factor is sensitive to changes of the quadrupole deformation. It is worth noting that, in general, the values of the parameter β affect twofold the form factor results. First, they define the set of the single particle WS wave functions for Eq. (13) and energies ϵ_{ps}^0 of Eq. (15) and, second, through the single-particle energies ϵ_{ps}^0 and the subsequently given pairing strengths, they determine the values of the orbit occupancies V_{pi}^2 entering Eq. (13).

In the next part of our work, for each isotope studied we investigated the influence of pairing correlations and deformation on the details of the nuclear surface indicated by the occupancies of the active orbits and the Fermi sea depletion (the sum of the valence vacancy numbers, U_{pi}^2). In Fig. 3, the proton-orbit occupancies versus the single particle energies are illustrated (cases denoted as WS and WS+BCS) and in Table 2 (last column) we report the Fermi sea depletions estimated for the case WS+BCS of Fig. 3. From these results we conclude that, the largest depletion corresponds to ^{24}Mg nucleus (the most deformed isotope of our set) and the smallest one to ^{32}S (the least deformed isotope of our set) which might be accidental. Concerning the two Mg isotopes, evidently, the depletion of the less deformed ^{26}Mg is appreciably smaller than that of ^{24}Mg showing the quite strong effect of

Table 1: The experimental values of the quadrupole moment Q and the corresponding values of the deformation parameter β taken from Ref. [26].

| Nucleus | Z | r_c (fm) | Q (barn) | β |
|------------------|----|------------|---------------------------|---------------------------|
| ^{24}Mg | 12 | 3.126 | $-0.16 \rightarrow -0.29$ | $0.38 \rightarrow 0.69$ |
| ^{26}Mg | 12 | 3.083 | $-0.11 \rightarrow -0.21$ | $0.27 \rightarrow 0.51$ |
| ^{28}Si | 14 | 3.177 | $+0.16 \rightarrow +0.18$ | $-0.31 \rightarrow -0.35$ |
| ^{32}S | 16 | 3.282 | $-0.12 \rightarrow -0.18$ | $0.19 \rightarrow 0.29$ |

deformation on the smearing of the nuclear surface. This result agrees with the "hardening" of the valence-proton distribution found in Ref. [13] which is due to the addition of two extra neutrons.

In Table 2, for comparison, we quote the shell model Fermi sea depletions of Refs. [13, 14] discussed in conjunction with elastic scattering data that provide information about differences in occupations of individual orbits between the pairs of neighboring even-even nuclei (^{24}Mg , ^{26}Mg) and (^{26}Mg , ^{28}Si). In this Table we also include the shell model Fermi sea depletion calculations of Ref. [33] and the values extracted from the experimental data of Refs. [34, 35]. The authors of Ref. [33], using two well-tested effective two-body interactions [36, 37] and treating the above nuclei as spherically symmetric systems, found drastically smaller depletions compared to ours and appreciably smaller than the experimental ones and those of Ref. [13]. From Table 2 one can infer that, the experimental Fermi sea depletions of Ref. [34, 35] are overestimated by about 40-130 % (depending on the nuclear system) from our method, and they are underestimated by about 10-50 % from the latter shell model calculations. The calculations of Ref. [13], in general, agree quite well with the experimental results.

The disagreement between these experimental data and our theory might be related to the factors discussed below, after making the following remarks:

Table 2: Fermi sea depletions for the deformed nuclear isotopes ^{24}Mg , ^{26}Mg , ^{28}Si and ^{32}S evaluated by the present work (last column) and previous spherical shell model calculations. The experimental results are from the following Refs. SM I [36], SM II [37], SM III [14], Exp. I [34] and Exp. II [35]. * This result comes from spherically symmetric Hartree-Fock calculations discussed in Ref. [14] which include the $0f_{7/2}$ orbital in the model space.

| Nucleus | Δ_{pp} (MeV) | SM I | SM II | SM III | Exp. I | Exp. II | This Work |
|------------------|---------------------|------|-------|--------|--------|---------|-----------|
| ^{24}Mg | 2.62 | 3.6 | 4.0 | 9.2 | 6.7 | 7.3 | 16.8 |
| ^{26}Mg | 2.52 | 4.3 | 3.9 | 6.7 | 5.8 | 6.0 | 12.6 |
| ^{28}Si | 2.43 | 6.9 | 6.8 | 9.8 | 10.7 | 10.7 | 15.3 |
| ^{32}S | 2.27 | 5.2 | 4.8 | 5.8* | 5.0 | 5.6 | 11.1 |

In our BCS treatment all orbits involved in our rich model space are considered as active, whereas the shell model results of Ref. [13, 33] originate from the very restricted model space $0d_{5/2}1s_{1/2}0d_{3/2}$ (both interactions used in [33] give rather similar orbit occupancies even though they differ in their predictions of occupancy dependent single particle energies, which means that for each isotope, the corresponding to our Fig. 3 pictures given by the latter two shell model calculations might be substantially different compared to each other). The parameterization of the deformed WS potential assumed in this paper, had originally been proposed for spherical nuclei (ranging from ^{16}O to ^{208}Pb). The confidence level of this parameterization (and subsequently of our results for deformed nuclei) relies upon its isospin-dependence characteristic which has indirectly been checked from the reliability of descriptions done (under the same assumptions with the present work) in Ref. [5, 28, 29].

In order to elucidate further the relationship between the deformation parameter β and the depletion of the valence shells, we have carried out a set of calculations with different values of β (originated from Ref. [26], see also Table 1) keeping fixed the pairing gap for the proton-proton and

neutron-neutron channel, $\Delta_{pp} = \Delta_{nn}$, in the BCS procedure (restricting in this way as much as possible the variation of pairing correlations effects). We have chosen the nuclei ^{24}Mg and ^{32}S and the results are displayed in Fig. 4. It is evident from this figure, that the Fermi sea depletion decreased slightly as the deformation effects tend to be canceled out and vice versa. More precisely the depletion ranging in the case of ^{24}Mg from 17% ($\beta = 0.38$) to 17.5% ($\beta = 0.69$) and in case of ^{32}S ranging from 11.11% ($\beta = 0.19$) to 11.31% ($\beta = 0.29$). This is an interesting result and may be accounted for as follows. By keeping the pairing interaction rather constant, a decrease of the deformation increases the orbit vacancies U_{pi}^2 and subsequently causes more effective participation of the nuclear core to the surface texture. Moreover, since for the latter results (and those of Table 2) we have not considered other sorts of correlations except pairing ones, the smearing of the Fermi surface is artificially interpreted by increasing the vacancies of the hole states (nuclear core), namely the Fermi surface depletion. In the region of deformation parameter, $0.2 \leq \beta \leq 0.7$, where our method is applicable, the Fermi sea depletion seems, for this reason, to be overestimated. At this point we should mention that, in the recent literature [19] authors assert that the depopulation of states below the Fermi energy is much more pronounced than it was believed in the past, since the quantitative information we have today from both theory and experiment support occupation probabilities in finite nuclei of the order of 75 % only. Our present results underly this result and it is expected from future measurements on specific nuclei with higher precision and covering larger range of momentum transfer to shed more light on the situation.

Before closing we note that, in our calculations, effects like finite proton size, center-of-mass corrections, etc., have not been taken into account. Instead, we restricted ourselves to the evaluation of the point nucleons (protons) distribution, which is equivalent to ignoring their internal substructure. This approximation has extensively been used in nuclear structure methods based on BCS ground state, because, the shape of the charge form factor is mainly determined by the shape of the point-proton density. In the present work we have also stayed within the assumptions of the above approximation encouraged for it by the rather well description of decay processes like the double beta decay [29] performed recently by using wave functions constructed as described in Sect. 2. As it is well known, the nuclear structure details affect considerably the corresponding double beta decay rates since its transition matrix elements are fairly sensitive.

4 Summary and Conclusions

In the present paper, at first, we formulated on the basis of BCS quasi-particles a simultaneous consideration of deformation and pairing correlations phenomena. The mean field description is provided in terms of an axially symmetric Woods-Saxon potential whereas for the two-body interaction we assumed schematic forces. Next, we tested this method by studying gross ground state properties like the nuclear form factor, the occupancy (vacancy) numbers of the active orbitals, and the corresponding depletion of the Fermi sea for the set of deformed nuclei, $^{24}_{12}\text{Mg}$, $^{26}_{12}\text{Mg}$, $^{28}_{14}\text{Si}$ and $^{32}_{16}\text{S}$. As it is well known from nuclear structure calculations, the focus on such primary gross properties, which is by itself a continuously important subject of study, provides very good tests for microscopic descriptions of the nuclear dynamics within many-body theories. This is encouraged by the great resource of data for these properties provided mainly by electron scattering experiments.

From the conclusions extracted out of the present calculations, we see that the use of deformed Woods-Saxon field in our BCS approach reproduces quite well the experimental form factor data in the set of isotopes studied, considerably better than the description offered when utilizing a deformed harmonic oscillator basis. The simultaneous consideration of the deformation and pairing correlations affect largely the Fermi sea depletion and produces appreciable smearing of the nuclear surface.

The investigation of the influence of the quadrupole deformation (parameter β) on the surface textures of the above moderately deformed nuclear systems, showed that the active orbit occupancies and, subsequently, the depletion of the Fermi sea for each isotope, are dependent slightly upon the parameter β . The results found for the Fermi sea depletion are more than 40% (depending on the specific nuclear system) larger than those emerging out of the old experimental data, from which one would infer that our method overestimates, somehow, the Fermi sea depletion through stronger deformation effects in order to compromise for the correlation effects not considered by it. However, recent information (experimental and theoretical) tend to support larger depletions (of the order of 20-25 %) which are consistent with our present estimations. The remaining discrepancy may be clarified from specific future experiments of greater precision and larger momentum transfers.

The authors would like to thank Professor I. Sick for providing us with the

experimental data for the charge form factor. One of the authors (Ch.C.M) would like to thank Professor S.E. Massen for useful comments and discussions. This work has been supported in part (TSK) by the IKYDA-02 project.

References

- [1] J. Suhonen and O. Civitarese, Phys. Rep. **300** (1998) 123.
- [2] F. Šimkovic and A. Faessler, Prog. Part. Nucl. Phys. **48** (2002) 201 and references therein.
- [3] R. Nojarov, Z. Bochnacki, and A. Faessler, Z. Phys. **A 324** (1986) 289.
- [4] P. Sarriguren, E. Moya de Guerra, and A. Escuderos, Phys. Rev. **C 64** (2001) 064306 and references therein.
- [5] F. Šimkovic, Ch.C. Moustakidis, L. Pacearescu, and A. Faessler, Phys. Rev. **C 68** (2003) 054319.
- [6] T.S. Kosmas, A. Faessler, and R. Sahu, Phys. Rev. **C 68** (2003) 054315.
- [7] A.N. Antonov, P.E. Hodgson, and I.Zh. Petcov, Nucleon Correlations in Nuclei, Springer -Verlag, (1993).
- [8] T.S. Kosmas, Nucl. Phys. **A683** (2001) 443.
- [9] P. Papakonstantinou, E. Mavrommatis, and T.S. Kosmas, Nuc. Phys. **A 713** (2003) 81.
- [10] S.E. Massen and Ch.C. Moustakidis, Phys. Rev. **C 60** (1999) 024005; Ch.C. Moustakidis and S.E. Massen, Phys. Rev. **C 62** (2000) 034318.
- [11] B.B.P. Sinha, G.A. Peterson, R.R. Whitney, I. Sick, and J.S. McCarthy, Phys. Rev. **C 7** (1973) 1930; G.C. Li, M.R. Yearian, and I. Sick, Phys. Rev. **C 9** (1974) 1861.
- [12] H. de Vries, C.W. de Jager and C. de Vries, At. Data and Nucl. Data Tables **36** (1987) 495.
- [13] R. Soundranayagam et al., Phys. Lett. **B 212** (1988) 13.
- [14] J. Wesseling et al., Nucl. Phys. **A547** (1992) 519; Phys. Rev. **C 55** (1997) 2773.
- [15] M. Bender, P.H. Heenen, and P.G. Reinhard, Rev. Mod. Phys. **75** (2003) 121.

- [16] J.A. McNeil, C.E. Price, and J.R. Shepard, Phys. Rev. **C 42** (1990) 2442.
- [17] T.S. Kosmas and J.D. Vergados, Nucl. Phys. **A536** (1992) 72.
- [18] L. Lapikas, Nucl. Phys. **A553** (1993) 297c.
- [19] V.R. Pandharipande, I. Sick, and P.K.A. de Witt Huberts, Rev. Mod. Phys. **69** (1997) 981.
- [20] W.A. Richter, B.A. Brown, Phys. Rev. **C 67** (2003) 034317.
- [21] J. Schwieger, T.S. Kosmas, and A. Faessler, Phys. Lett. **B 443** (1998) 7.
- [22] D. Van Neck, M. Waroquier, V. Van der Sluys, and J. Ryckebusch, Phys. Lett. **B 274** (1992) 143.
- [23] D.G. Madland and J.R. Nix, Nucl. Phys. **A476** (1988) 1.
- [24] P. Möller, J.R. Nix, W.D. Myers, and W.J. Swiatecki, At. Nucl. Dat. Tabl. **59** (1995) 185.
- [25] G.A. Lalazissis, S. Raman, and P. Ring, At. Nucl. Dat. Tabl. **71** (1999) 1.
- [26] N.J. Stone, Oxford University, preprint (2001).
- [27] Y. Tanaka, Y. Oda, F. Petrovich, and R.K. Sheline, Phys. Lett. **83B** (1979) 279.
- [28] P. Sarriuguren, E. Moya de Guerra, L. Pacearescu, A. Faessler, F. Šimkovic, and A.A. Raduta, Phys. Rev. **C 67** (2003) 044313.
- [29] F. Šimkovic, L. Pacearescu, and A. Faessler, Nucl. Phys. **A733** (2004) 321.
- [30] S.G. Nilsson and I. Ragnarsson, Shapes and Shells in Nuclear Structure (Cambridge University Press, 1995).
- [31] V.G. Soloviev, Theory of complex nuclei, Pergamon press, 1976, pp. 111.
- [32] J. Praena, E. Buendia, F.J. Gálvez, and A. Sarsa, Phys. Rev. **C 67** (2003) 044301. E. Buendia, F.J. Galvez, J. Praena, and A. Sarsa, J. Phys. **G 26** (2000) 1795.
- [33] V. Potbhare and N. Tressler, Nucl. Phys. **A530** (1993) 171.
- [34] V. Potbhare and S.P. Pandya, Nucl. Phys. **A256** (1976) 253.
- [35] B.S. Ishkhanov, I.M. Kapitonov, and A.V. Shumakov, Nucl. Phys. **A394** (1983) 263.
- [36] B.H. Wildenthal, Prog. Part. Nucl. Phys. **11** (1984) 5.

[37] B.M. Preeodom and B.H. Wildenthal, Phys. Rev. **C 6** (1972) 1633.

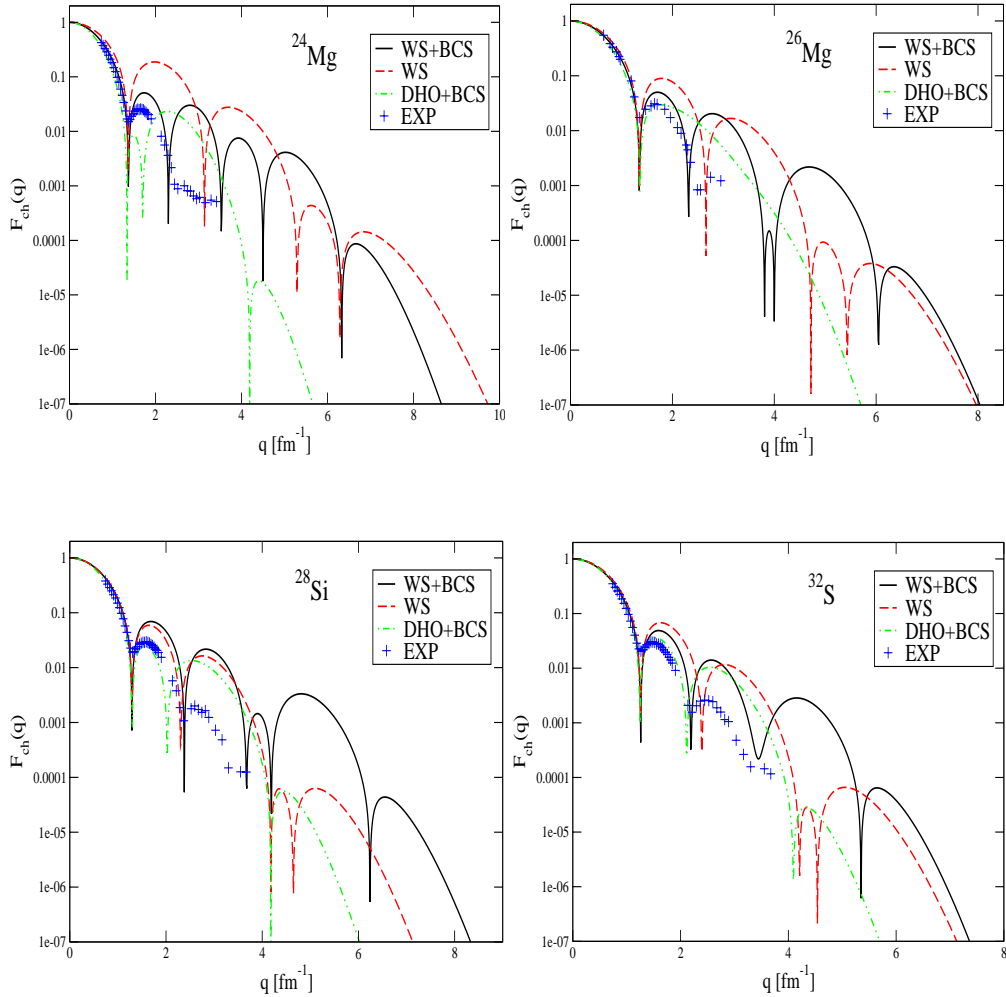


Figure 1: Calculated and experimental [11, 12, 13, 14] charge form factors for the deformed nuclei ^{24}Mg , ^{26}Mg , ^{28}Si and ^{32}S . The results labeled WS+BCS (solid line) include pairing correlations and deformation effects while those labeled WS (dashed line) originate from a simple Slater determinant constructed out of a deformed Woods-Saxon basis wave functions. The dashed dotted curve, DHO+BCS, comes from a deformed harmonic oscillator field employed in the BCS ground state.

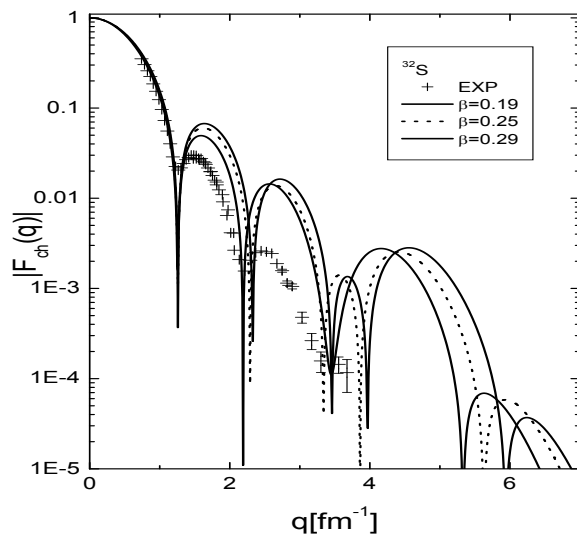
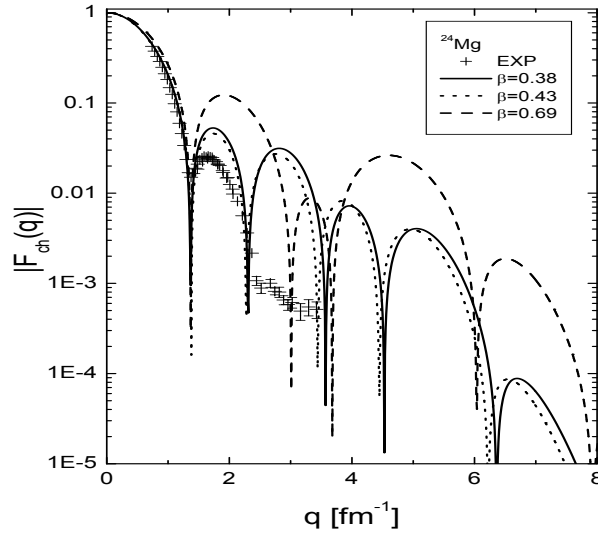


Figure 2: Charge form factor of ^{24}Mg (up) and ^{32}S (down) for various values of the deformation parameter β entering the deformed WS basis. Pairing correlations are also taken into consideration through the BCS ground state. The values of β comes from Ref. [26].

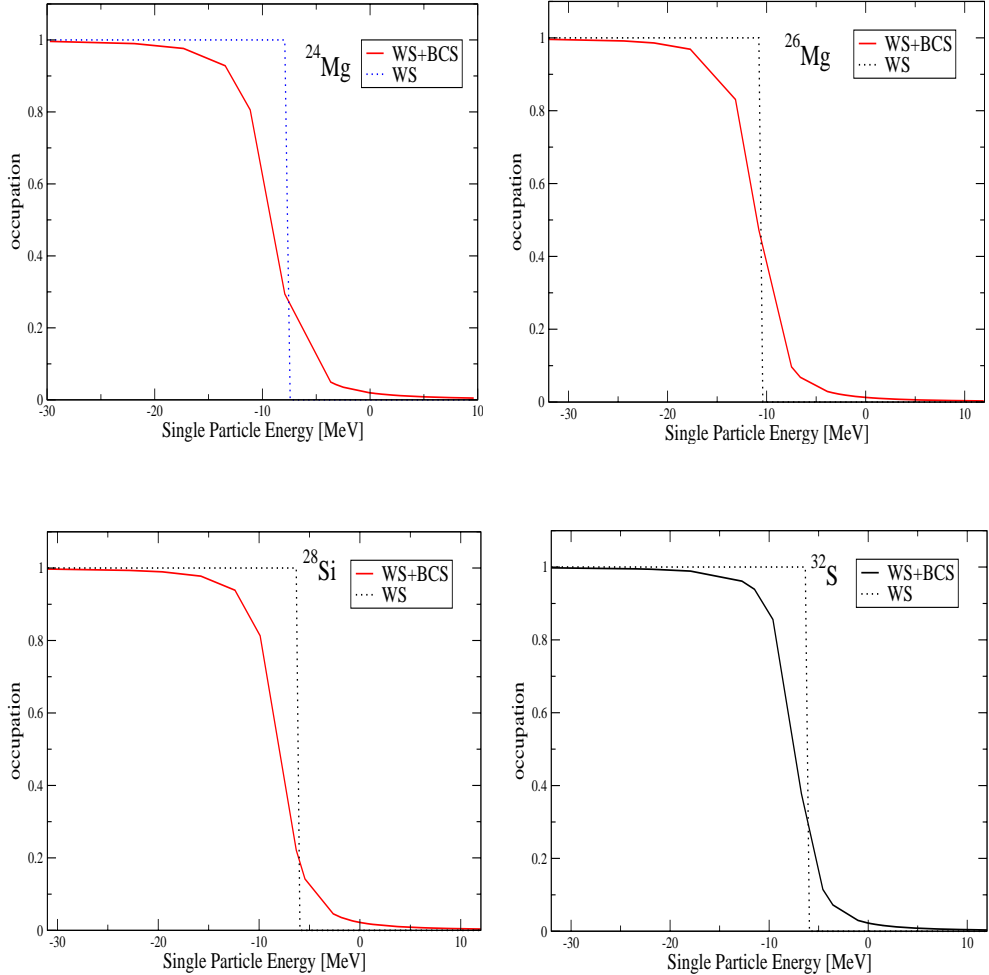


Figure 3: Proton occupation probabilities near the Fermi surface for the nuclei ^{24}Mg , ^{26}Mg , ^{28}Si and ^{32}S . The diffuseness of the Fermi surface reflects the pairing correlations and deformation effects. The notation is the same with that of Fig. 1.

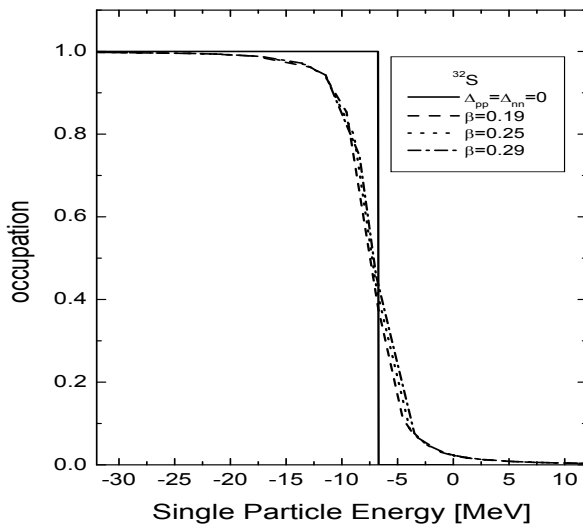
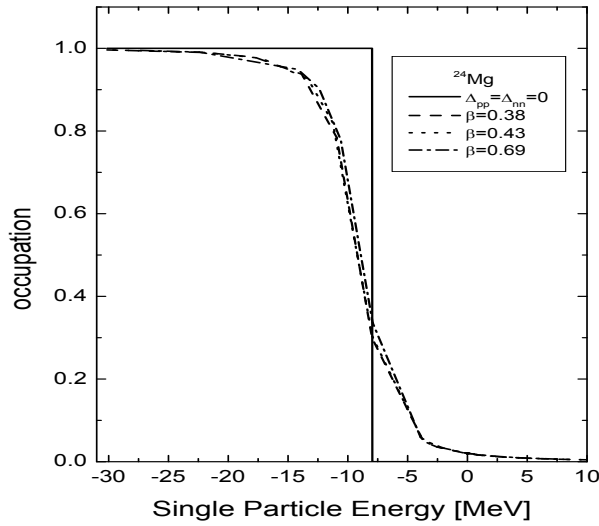


Figure 4: The diffused Fermi surface and the Fermi sea depletion for ^{24}Mg (up) and ^{32}S (down) produced by varying the deformation parameter β in a deformed Woods-Saxon basis (see Table 1). The strength for proton-pair (neutron-pair) interaction in the BCS procedure is fixed at the value $\Delta_{pp} = \Delta_{nn} = 12.84/A^{1/2}$ MeV.